Nonlinearity in the Light Processing of the Human Visual System

Ioannis Petridis, MSc Biomedical Engineering, 3ME Faculty, Delft University of Technology

***Abstract*—Visual evoked potentials, i.e responses to visual stimulation as recorded using electroencephalography have indicated the existence of nonlinear behavior of the visual pathway. Nonlinearities and time delay in the visual system play an important role in understanding the complex nature of the visual system. This study investigated the nonlinear interactions and time delay in the visual pathway, using several types of stimulation paradigms. Multisine (i.e sum of multiple sinusoidal signals) and sine light stimulation were presented to healthy participants in order to elicit steady-state visual evoked responses. The recorded signals were analyzed using multi-spectral phase coherence, a novel cross-frequency phase coupling metric, in order to quantify the nonlinear interactions, form a brain map and estimate time delay. Chirp light stimulation (signals with linearly increasing frequencies) was used to elicit visual responses inside a specific frequency range. Time delay was estimated using Fractional Fourier Transformation due to its ability to handle chirps' non-stationary properties. Brain maps indicated that multisine paradigms elicit more localized nonlinear interactions than chirp paradigms. All sinusoidal stimulation provided clusters of similar time delays. Bisine presented the most distinctive groups, fact that suggests that bisine is able to be used as a distinction measure. Trisine time delay showed the lowest variance, fact that shows more accurate estimation. Chirp time delay presented also small variances but the mean time delay found to be very frequency dependent. To conclude, this study showed that multisine paradigms are suitable to be used to elicit nonlinear responses but time delay may not be sufficient measure to fully describe the visual system.**

Keywords*—Nonlinear; visual system; steady state visual evoked potentials; light stimulation; light processing; EEG analysis; brain dynamics; sinusoidal; chirp; multisine.

I. Introduction

Vision involves communication within and between several parts of the brain, involving retina, optic chiasm and optic tracks, thalamus and visual cortices [1][2]. During visual processing, the external visual input is communicated among these regions by neural synchronization. Firing of neurons inside the different structures is synchronized in order to pass and process the external input [3]. Neural synchronization has linear [4][5] and non-linear components due to synapses and firing mechanisms which are highly nonlinear [6][7][8]. The propagation of the stimulation signal through this entire pathway is not instantaneous, but has a measurable time delay. Nonlinear interactions and timing are key to understand the complexity of the visual system and play an important role in the integration and interpretation of visual input [9][10][11]. The quantification of the time delay can be a distinguishing factor between a healthy and diseased visual system suffering from disorders like migraine, epilepsy etc.

Linear interactions describe the neural relation at the same frequency (e.g $f_1 \rightarrow f_1$), while in nonlinear synchronization, interactions can occur at harmonic frequencies (e.g $f_1 \rightarrow 4f_1$) and at intermodulated frequencies (e.g $f_1, f_2 \rightarrow 3f_1 + 4f_2$). Figure 1 illustrates this difference [10]. Harmonics are integer multiples of the input frequencies and show how neural processing resonates [12], while intermodulation is linked to the contribution of multiple input frequencies to the output and shows the extend of the integration among those frequencies [13].

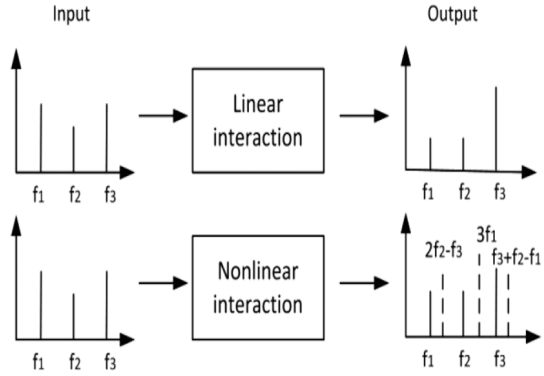

Fig. 1: Difference between a linear and a nonlinear system in frequency domain. The solid lines in the output correspond to the linear interactions, showing that the system generates output at the same frequencies as input. The dashed lines correspond to the nonlinear interactions, indicating that the system generates output at non-stimulated frequencies as well [10].

Nonlinear interactions can occur at different orders (n-orders) of nonlinearity. In a 2^{nd} order nonlinear system for example, with 7 Hz input frequency, it is expected that the output will present power at 7 Hz and 2*7=14 Hz, while in a 3^{rd} order there will be power at 7 Hz, 2*7=14 Hz and 3*7=21 Hz. Since the order of visual system was shown to be beyond the second [14][15][16], there is a need for a measure that can detect and handle high order nonlinear interactions during visual stimulation. Multi-spectral phase coherence (MSPC), as described by Yang et al. (2015), is able to provide a robust way to quantify nonlinear coupling among input frequencies and hence detect nonlinear interactions [10][17]. The measure can also estimate the time delay between the input and output [10]. Therefore it provides knowledge regarding the propagation time of the stimulation signal in the visual pathway. To

fully use the strengths of MSPC a proper input signal with certain frequencies set should be selected [10]. This signal should be able to elicit distinctive responses in harmonics and intermodulated frequencies. The best way of achieving this is the multisine input signal, i.e the sum of multiple sinusoidal signals. Because of its ability to concentrate power in specific and finite set of frequencies and to evoke steady-state responses in harmonics and intermodulated frequencies, periodic multisine stimulation constitutes an exemplary type of stimulus for a system's nonlinear investigation [18].

Visual input presented to the retina activates, after processing in the above described pathway, the visual cortex. There, the brains response can be captured with the use of electroencephalography (EEG). A common way to generate brain activity in the visual pathway is by flickering light. The elicited brain activity is called visual evoked potential (VEP), an effective tool for the study of vision perception [19].

The frequency content and the shape of the VEP changes according to the stimulation characteristics. Four types can be distinguished, separated in two major categories: 1) transient visual evoked potential (TVEP); and 2) steady-state visual evoked potential (SSVEP). A TVEP is generated in response to a sudden stimulus [20] while SSVEPs are formed in the presence of a longer repetitive stimulus [21]. Two types of SSVEP stimulation are i) multisine; and ii) chirp. The multisine signal is formed by the summation of two or more sinusoidal signals with stable frequencies over time. The chirp signal has linearly incrementing frequency, forming thus a swiftly changing signal inside a specific frequency range [22][23].

Time delay of the visual system can be an important marker for characterizing the visual system dynamics in case of visual system related disorders. However it is still unknown if the different types of stimulation result in different time delay estimations. Also, different regions of the brain might be activated in response to e.g. multisine and chirp stimulation. For this study, we quantified and compared the visual system's time delay and activation patterns using different types of stimulation paradigms.

II. Methods

A. Subjects

Twelve healthy volunteers, six men and six women aged 24 $\pm$ 3 years participated in the experiment. The experimental procedure was approved by the Human Research Ethics Committee of the Delft University of Technology. All participants signed informed consent, filled in a questionnaire regarding their gender, sleep, menstrual cycle and light sensitivity, and received financial compensation for the time offered to the experiment.

B. Light Protocol

Eight stimulation paradigms were designed to elicit visual evoked potentials (SSVEP). The paradigms can be separated into four categories, 1) single VEP; 2) one frequency sinusoidal (sine); 3) multiple frequencies sinusoidal (multisine); and 4) linearly increasing frequency sinusoidal (chirp) stimulation paradigms.

Single VEP paradigm consisted of 100 repetitive light flashes appearing in random intervals within 0.8 - 1.2 Hz. The purpose of this stimulation was to help subjects become acquainted with the flickering light. The stimulation lasted 2 minutes.

The second category consisted of one-frequency sinusoidal stimulations. In total, three sines were used with frequencies of 7, 13 and 23 Hz. Ten blocks of 32 repetitions (1 second per repetition) were presented with 5-10 seconds break in-between blocks (stimulation time: seven minutes per frequency), providing 320 trials per frequency.

The third category consisted of a double sinusoidal (bisine: sum of two frequencies of 13 and 23 Hz) and a triple sinusoidal (trisine: sum of three frequencies of 7, 13 and 23 Hz) stimulation paradigms, presented also in ten blocks of 32 repetitions. All sinusoidal signals had random phases and the chosen frequencies prevented second and third order overlap in harmonic and intermodulation frequencies.

The last category consisted of two chirp signals with large frequency range. The first range was between 10 and 40 Hz with 3 Hz/s increasing frequency rate (10 seconds per block). The stimulation lasted four minutes. The second range was between 8 and 56 Hz with 6 Hz/s increasing frequency rate (6 seconds per stimulation block). The stimulation lasted three minutes. In both cases, 12 repetitions were presented with 5-10 seconds breaks in between.

C. Equipment and experimental setup

Participants were instructed to sit comfortably and steadily in a chair located in a dark, quiet and electromagnetic shielded room. Visual stimuli were presented using a pair of red-colored light emitting diode goggles placed in front of the subjects' eyes. Stimulation protocols were transferred from Matlab (R2015a, Mathworks) to the goggles via a digital-to-analog converter (NI9265, National Instruments)

High density electroencephalogram (EEG) was recorded using a 128-electrode cap (5/10 system, WaveGuard cap, ANT Neuro) with Al/AgCl electrodes, an amplifier (Refa 136 electrodes, TMSi) and using the common average reference. The ground electrode was placed on the left mastoid and the electrodes' impedance was kept below 5 $k\Omega$. Two auxiliary ports were used to record the stimulation signal and trigger signal, to be used for data processing.

The experiment consisted of four phases. The first stage was to prepare the participant and connect the EEG equipment. The second stage was to record the resting state during which participants had their eyes closed and no stimulus was presented. The third stage was to apply transient VEP stimulation in order for the subjects to become acquainted with the flickering light. The last stage was to apply the different stimulation paradigms in random order. During the stimulation process, participants were asked to keep their eyes closed until told otherwise. Both preparation and stimulation periods lasted for one hour resulting in a two-hour experiment.

D. Analysis

1) Data pre-processing: The acquired data were imported in Matlab (R2015a, Mathworks) using scripts from EEGLAB

(version 13.6.5b, Swartz Center for Computational Neuroscience). Afterwards, the data were processed in Matlab using custom-written scripts. The recorded (raw) EEG data were filtered using a 4^{th}-order, zero-phase bandpass filter between 0.5 and 200 Hz and were cut, using the trigger signal, into 320 trials for (multi)sines and 12 repetitions for chirps. The next step was to remove artifacts like bad electrode movements and eye blinking which also exists in case of closed eyes. The artifact elimination was based on visual inspection of each trial for each stimulation and each subject. After careful inspection the rejection threshold was defined to be the mean plus-minus five times the standard deviation of the recording EEG. Following the artifact removal, the clean (multi)sine EEG data were reliable to be used for nonlinear phase coupling analysis [10] and the clean chirp EEG were averaged in order to be used for further analysis.

2) Signal to Noise Ratio: Before assessing the nonlinear interactions and calculating the time delay, the relative power of the EEG data was measured. This quantification helps to distinguish the signal from background noise, as any part of the recorded signal without the same period as the periodic stimulation signal can be regarded as noise [24].

Fast Fourier transform was applied to obtain the frequency domain representation $X(f)$ of the stimulation signal $x(t)$. The total power E_x was estimated by averaging $X(f)$ over the trials (P) and summing over all frequencies (F):

$$\hat{E_x} = \sum_{f=1}^{F} \left| \frac{1}{P} \sum_{p=1}^{P} X^P(f) \right|^2 \tag{1}$$

To retrieve the noise level of the recorded signal (EEG), the variance over trials (P) and summing over all frequencies (F) was estimated:

$$\hat{\sigma_x}^2 = \sum_{f=1}^{F} \frac{1}{P-1} \sum_{p=1}^{P} \left| X^P(f) - \frac{1}{P} \sum_{p=1}^{P} X^P(f) \right|^2 \tag{2}$$

The Signal to Noise Ratio (SNR) for each electrode was obtained by dividing the estimate of power by the estimate of the noise level. The derived estimated was scaled by the number of periods in order to obtain the noise level in the averaged data [24]. Therefore the electrode with the strongest response could be distinguished:

$$SNR = \frac{\hat{E_x}}{\hat{\sigma_x}^2} \tag{3}$$

$$SNR_{scaled} = \frac{SNR}{P} \tag{4}$$

3) Multi-Spectral Phase Coherence (MSPC): Multi-Spectral Phase Coherence (MSPC) is a phase synchrony (coupling) measure introduced to describe the phase relation among the nonlinear neural interactions either for one or more frequencies based purely on phase information. It is able to detect both harmonic and intermodulation coupling and its independence of signals amplitudes constitutes it a reliable quantification [10]. Hence, we used MSPC to estimate nonlinear interactions and time delay for the different light stimulation paradigms (sines-multisines).

MSPC calculates high order nonlinear phase coupling using:

$$|\Delta\phi| = \left| \sum_{r=1}^{R} \alpha_r \phi(f_r) - \phi(f_\Sigma) \right| = const \tag{5}$$

where $f_1, f_2, ..., f_R$ the input frequencies, f_Σ the output frequency that is a combination of the input frequencies, $f_\Sigma = \sum_{r=1}^{R} \alpha_r f_r > 0$ (α_r are integers and $\sum_{r=1}^{R} |\alpha_r| = d$), d is the order of nonlinearity and $\phi(f)$ are the phases of input and output signals. Equation 5 covers all possible harmonics and intermodulation frequencies at any order of nonlinearity. Therefore, in the case of a triple frequency sinusoidal signal applied to a third order nonlinear system, the output frequencies will include harmonic and intermodulated components, i.e $3f_1, 3f_2, 3f_3, f_3f_2f_1, 2f_rf_m, f_r2f_m (r, m = 1, 2, 3, r \neq m)$. All the derived components are nonlinearly phase coupled to the input frequencies [10].

Multi-spectral phase coherency Ψ and estimated phase lag are defined mathematically as:

$$\Psi_{XY}(f_1, f_2, ..., f_R; \alpha_1, \alpha_2, ..., \alpha_R)_d = \frac{1}{K} \sum_{k=1}^{K} exp\left(j \left(\sum_{r-1}^{R} \alpha_r \phi_{X_k}(f_r) - \phi_{Y_k}(f_\Sigma) \right) \right) \tag{6}$$

$$\Delta\phi_{XY}^{(est)} = arctan(Im(\Psi_{XY})/Re(\Psi XY)) + 2p\pi \tag{7}$$

where f_i are the input frequencies of the Fourier transformed of a time series $x(t)$, f_Σ is the output frequency of the $Y(f)$ with k epochs, α_r are the weights of the input frequencies to output frequency with $\sum |\alpha_r| = d$, where d is the order of nonlinearity. The MSPC at order d is defined as the magnitude of Ψ and is denoted with ψ. MSPC value ranges between 0 and 1 reflecting respectively the randomness and consistency of the cross frequency phase difference between the epochs. In case of nonlinear relationship between the signals, MSPC can also indicate the neural interaction's direction, i.e the causality of the signals by calculating the contribution of the input frequencies on the prediction of the output frequency. For this case the notation $\psi_{X \to Y}$ is used to show the directionality.

Given a relationship like the directionality $(X \to Y)$, the time delay between light input X and and visual evoked response Y can be estimated by:

$$\tau_{est} = \min_{\tau > 0} \left(\sum_{f_\Sigma = \sum_{r=1}^{R} \alpha_r f_r} \left| exp\left(j(2\pi f_\Sigma \tau) - \frac{\Psi_{XY}(f_1, f_2, ..., f_R, \alpha_1, \alpha_2, ..., \alpha_R)}{\psi_{XY}(f_1, f_2, ..., f_R, \alpha_1, \alpha_2, ..., \alpha_R)} \right) \right| \right) \tag{8}$$

We computed $\psi_{stimulation \to EEG}$ up to the third order, since the frequencies of the stimulation (7, 13, 23 Hz) allow the study of the interactions without an overlap of harmonic and intermodulation components. In addition, topographical plots were calculated in order to identify the region of the brain that is activated.

4) Time Delay Selected Range and Expected Values: The selected range for the time delay estimation was 50 to 150 ms, based on literature showing delays of about 120 ms for 8-15 Hz stimulation and about 60 ms for 15-30 Hz [15][25]. Moreover, a theory regarding the existence of three frequency components in steady-state visual evoked potentials has stated the time delay between 25-60 Hz is about 30-60 ms, between 15-25 Hz is about 85-125 ms and below 15 Hz is above 130 ms [15][20][26]. Those components however, are not always observed and are not yet fully understood. Therefore their boundaries are subjective to changes.

5) Fractional Fourier: The fact that FT decomposes the chirp signal into oscillatory functions, constitute FT incompetent for the analysis of chirp signal's non-stationary nature. Instead $FrFT$ was selected because it decomposes the chirp signal into chirp functions, providing thus a compact representation of the signal in a different u-domain [27].

The chirp signals [22] are described by the following formula:

$$s(t) = \sum_{k=1}^{N} A_k cos(2\pi k f_0 t + \pi \lambda t^2) + n(t) \tag{9}$$

with central frequency f_0, chirp rate λ, amplitude of each harmonic A_k, number of harmonics N, artifacts and noise of background EEG activity $n(t)$.

The time-frequency representation of the chirp is a straight inclined line forming an angle α with the time axis. The angle α corresponds to the chirp rate of the chirp signal [22][27][28]. During $FrFT$ the time-frequency distribution is rotated and when the angle α becomes equal to $-arcot(\lambda)$ then the $FrFT$ of the chirp is a distinctive impulse response exactly on the central frequency of the chirp signal [22]. $FrFT$ is considered to be a generalization of the classical FT since it behaves like FT when the rotation angle is multiple of $\pi/2$ [22].

We computed $FrFT$ for the chirp signals and we estimated the phase lag and the linear time delay between the chirp stimulation $x(t)$ and the chirp VEP $s(t)$ by:

$$\phi_d(\omega) = arg\left[\frac{S(e^{j\omega})}{X(e^{j\omega})}\right] \tag{10}$$

$$\tau = -\frac{d[\phi_d(\omega)]}{d\omega} \tag{11}$$

The linear time delay can be obtained by taking into account the fundamental components of $S(e^{j\omega})$ and $X(e^{j\omega})$ and create a linear fit between them.

E. Complications

The major complication we faced, was the existence of an artifact in the raw EEG data of the first six participant as depicted in figure 2. The artifact was the result of the contamination of the EEG signal due to the trigger signal. As can be seen the artifact is present at the first 25 samples of the recordings and its effect in the calculated parameters was high. To remove the artifact the method of linear interpolation was used for the replacement of the 25 samples. Comparison of six subjects with and without artifact was made in order to justify the validity of this method, also given in the Appendix A.

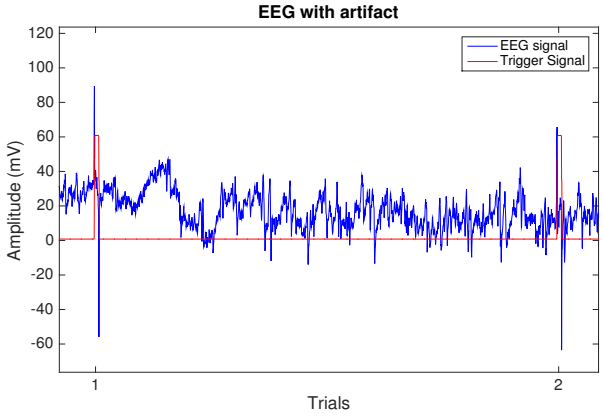

(a) Trials

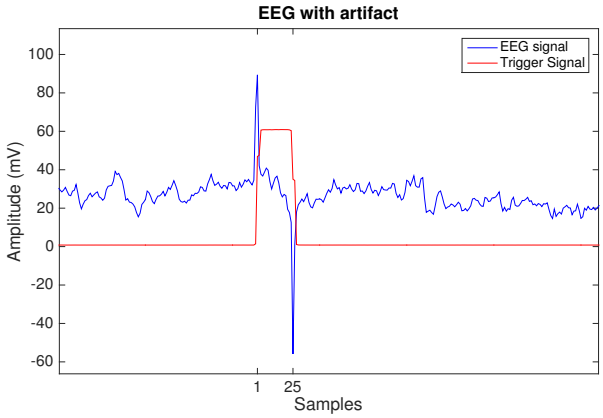

(b) Samples

Fig. 2: EEG signal of one channel and trigger signal responsible for the artifact. a) Shows that the artifact happens in the beginning of each trial. b) Shows the position of the artifact in each trial.

III. Results

This section presents

- The averaged SNR over all subjects for a representative stimulation type.
- Averaged topographical plots of MSPC values showing the magnitude of the nonlinear interactions for a representative stimulation type.
- Averaged topographical plots of different order of MSPC for a representative stimulation type.
- Time delay estimations for different stimulation types

A. (Multi)sines

1) Signal to Noise Ratio: Signal to noise ratio was calculated over 320 trials before removing the artifacts in order to obtain an indication of the brain's activity in the presence of light stimulation. The periodic response of the brain is illustrated by the highest SNR values [24]. Figure 3-a demonstrates the averaged SNR over all subjects for double sinusoidal (bisine) stimulation. The highest SNR can be found in between the parietal and occipital lobes. Specifically electrodes PPO1, Pz, PPO2, PP04h, Oz, PPO3h, POz show a higher brain activation inside this area.

2) Multi-spectral Phase Coherence (MSPC): Having already an indication of the brain's activated regions, multispectral phase coherence was calculated in order to quantify the nonlinear interactions between the stimulation and response. MSPC was applied on clean data. Figure 3-b demonstrates the averaged $\Psi_{stimulation \rightarrow EEG}$ over all subjects for bisine stimulation. The higher MSPC values can be found in the same area where SNR is maximum, i.e the parietal and occipital lobes. MSPC values are more localized than SNR values, showing that significant nonlinear interactions are more dominant and acute at the visual area.

Second and third order harmonic and intermodulation coupling between the stimulation and the response was detected. Figure 4 depicts the magnitude of the coupling for a representative subject, the mean MSPC and the standard error of the mean for all subjects at POz electrode, proving the existence of significant nonlinear interactions.

The examined orders activate different parts of the brain. The fundamental frequencies activate the occipital lobe while the second and third order harmonics and intermodulation frequencies seems to affect more the parietal lobe. The higher order of interest, the more localized the brain activation is as can be seen in figure 5 a, c and e. Comparing multisines and single sines responses, the localization of the multisine response in any order seems to be more robust than sine responses that seem to activate more brain regions. An example of representative stimulations can be observed in figure 5.

3) Time Delay: SNR and MSPC take their maximum value at POz electrode, located on the visual cortex. Therefore the same electrode was selected to calculate and compare time delays among all (multi)sines paradigms. A summarized graph of the time delay can be seen in figure 9-a

There is not a clear outcome regarding the time delay with respect to the stimulation types just by observing the values in figure 9-a. The values ranged from 50 to 150 ms without a specific pattern. Only for bisine time delay, three clusters are highly distinguishable. The first consists of the participants P2, P3, P7, P8, P9, P10 with time delay equal to 52 ± 2 ms, while the second consists of the participants P4, P5, P6, P11, P12 with time delay equal to 133 ± 4 ms. The third one consists only from participant P1 with time delay equal to 94 ms. Based on this clustering, the MSPC values contributing in each time delay for all stimulation types, are plotted in Appendix G verifying the existence of clusters in all (multi)sine paradigms. Bisine presents the stronger clustering.

To further prove the existence of the three clusters (components) defined by Regan (1989) and explained by Vialatte et al. (2010) [20][29], the mean MSPC values for each component

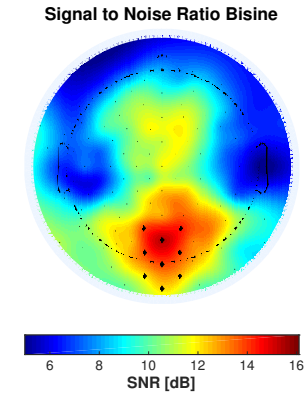

(a) SNR

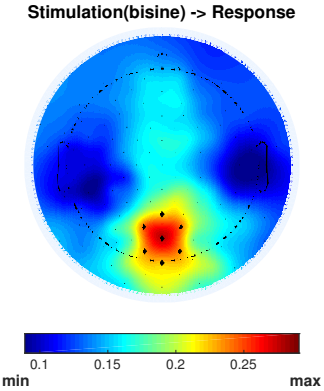

(b) MSPC

Fig. 3: a) Signal to noise ratio (SNR) per electrode averaged over all subjects. The highest SNR is found between parietal and occipital brain regions. b) Average of normalized topography of MSPC magnitude over the subjects. MSPC values are normalized in each electrode by dividing over the maximum for each subject before computing the average. Thus the contributions of each subject is equalized. Black dots indicate the electrodes' locations.

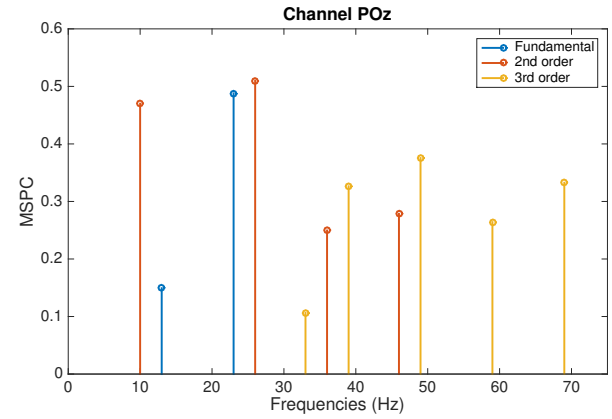

(a)

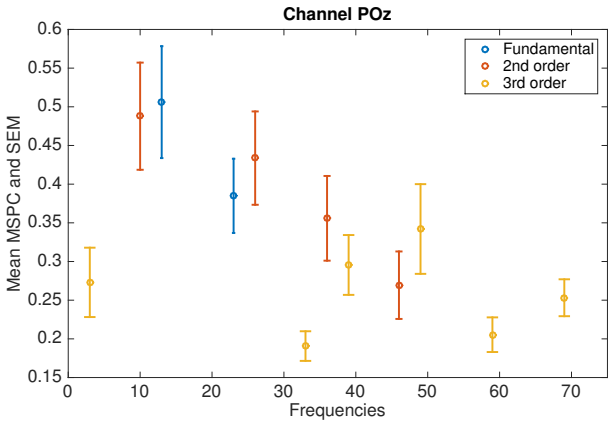

(b)

Fig. 4: a) Nonlinear interaction between the stimulation and EEG signals for a representative subject using bisine stimulation. b) Mean and standard error of the mean averaged over all subjects for bisine stimulation. The result is shown for channel POz, which has the largest mean significant $\psi_{stimulation \rightarrow EEG}$. The fundamental frequencies are depicted with blue, the second order interactions (harmonic-intermodulation) with red and the third order interactions with yellow.

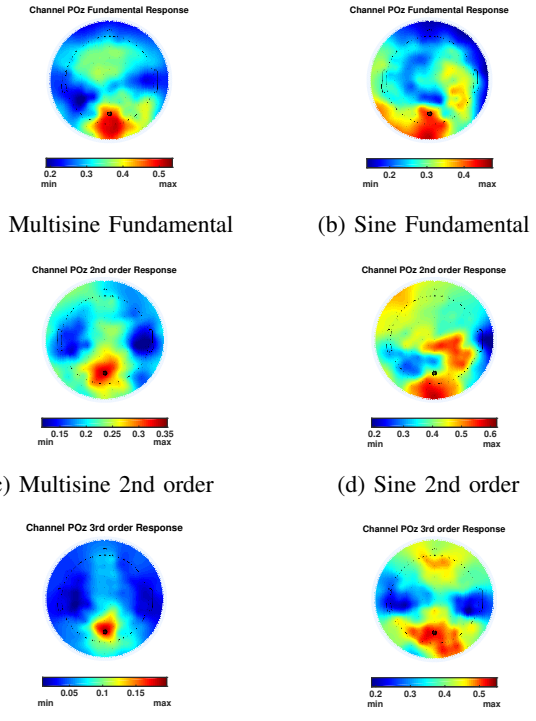

(a) Multisine Fundamental (b) Sine Fundamental

(c) Multisine 2nd order (d) Sine 2nd order

(e) Multisine 3rd order (f) Sine 3rd order

Fig. 5: Average of normalized topography of MSPC magnitude for different orders between a representative multisine (13-23 Hz) and a representative sine (7 Hz), over all subjects. MSPC values are normalized in each electrode by dividing over the maximum for each subject before computing the average, thus the contributions of each subject is equalized. a-b) Activation patterns of the fundamental responses; c-d) Activation patterns of the 2nd order responses; and e-f) Activation patterns of the 3rd order responses. The dots depict the electrode's position. The filled dot rerpesent the electrode with the highest MSPC value (POz) if all orders taken into consideration at the same time

was calculated and plotted against the time delay. It was expected that the higher the time delay (above 130 ms), the more prominent the interactions of the third component will be, while the lower the time delay (below 60 ms), the primary component will be more dominant. For time delays in between 60 and 130 ms the second components should present the higher interactions. By observing the figure 6 describing the multisine stimulations, can be seen that the aforementioned expectation partially is fulfilled.

4) Multisines vs Combined Sines: MSPC values were calculated for each sine separately. These values were later used to create two artificial stimulation paradigms. The first one is a combination of 13 and 23 Hz sines and the second of 7, 13 and 23 Hz sines. The combined MSPC values for each new paradigm were used to calculate time delay. The time delay estimations for the combined 13-23 Hz sines was found to be 106 $\pm$ 27 ms, while for the combined 7-13-23 Hz was found to be 92 $\pm$ 27 ms. The aforementioned values have significant differences when compared with the time delay for bisine (89 $\pm$ 41 ms) and trisine (121 $\pm$ 22 ms) respectively. Figure 9-b shows the time delays for each subject for multisines and combined sines paradigms.

B. Chirps

1) Signal to Noise Ratio: Figure 7 illustrates the chirp response characteristics in terms of signal to noise ratio (SNR). It can be seen that the chirp responses, similar to the multi(sine)

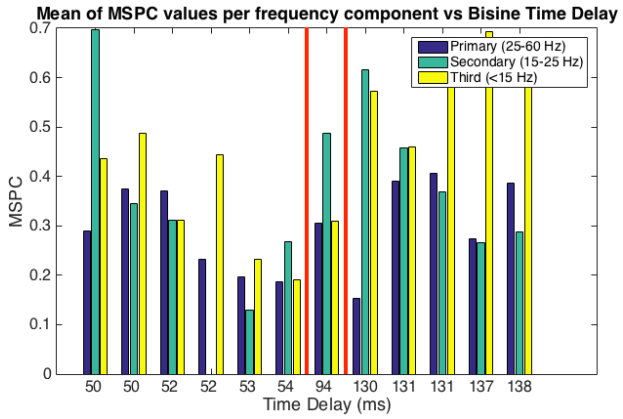

(a) Bisine

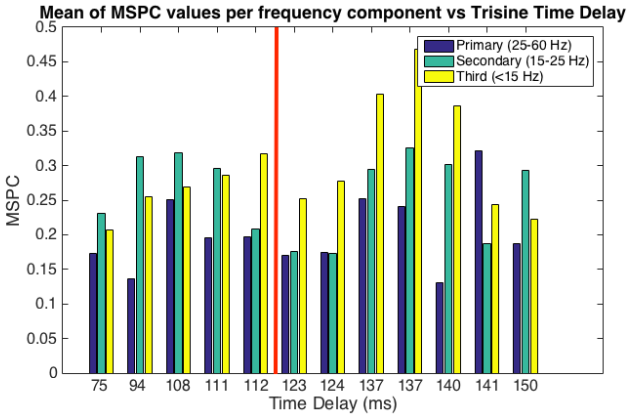

(b) Trisine

Fig. 6: Mean MSPC for each frequency component for multisine stimulations. Each value of time delay represents a subject. The vertical red lines divide time delay into groups

responses, are mainly processed in the occipital region, specifically around the electrodes POz, POO3h, POO4h, Iz, OI1h, OI2h, Oz. However the two chirp paradigms seem to follow different activation patterns.

2) Time Delay: SNR takes its maximum value at Oz electrode for chirp 10-40 Hz and at POz electrode for chirp 8-56 Hz, both located on the visual cortex. The time delay values of both electrodes for both chirp stimulations were taken into account. The difference in time delay for each electrode was 7 ms (89 ms at POz - 82 ms at Oz) for the 10-40 Hz stimulation and 3 ms (73 ms at POz - 70 ms at Oz) for the 8-56 stimulation. The difference in time delays for the two paradigms was 16 ms for POz and 12 ms for Oz. Since the difference in time delays for the two paradigms is only 4 ms between the two electrodes, POz electrode was selected as representative channel in order to keep up with the channel selection for the rest of the time delay calculations. Therefore electrode POz was selected to calculate and compare time delays among all paradigms.

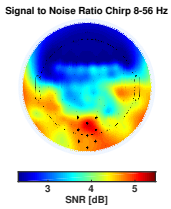

(a) Chirp 8-56 Hz

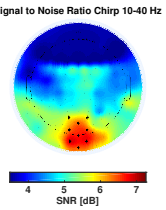

(b) Chirp 10-40 Hz

Fig. 7: a) Chirp 8-56 Hz; b) Chirp 10-40 Hz. Signal to noise ratio (SNR) per electrode averaged over all subjects. The highest SNR is found between parietal and occipital brain regions. Black dots indicate the electrodes' locations.

The time delays for chirp stimulation present also clustering phenomena. The 10-40 Hz paradigm consists of three clusters. The first consists of participants P1, P4, P7 with time delay equal to 117 $\pm$ 5 ms. The second consists of participants P10-P12 with time delay 66 $\pm$ 2 ms. The third one consists of the rest of the subjects with time delay 86 $\pm$ 7 ms. On the other hand, the 8-56 Hz paradigms consists of two clusters. The first consists of participants P1-P5, P8, P9 with time delay 81 $\pm$ 7 ms, while the second consists of the rest of the participants with time delay 61 $\pm$ 8 ms. A summarized graph of the time delay can be seen in figure 9-c.

Figure 8 summarizes the time delay for each stimulation paradigm over all subjects. Sines 13 and 23 Hz provide the lowest inter-subject variability. Trisine stimulation presents smaller variance compare to bisine.

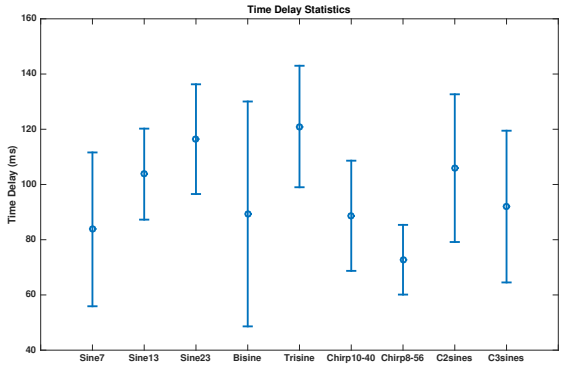

Fig. 8: Mean and standard deviation of the time delay per stimulation type. All time delays are calculated for channel POz.

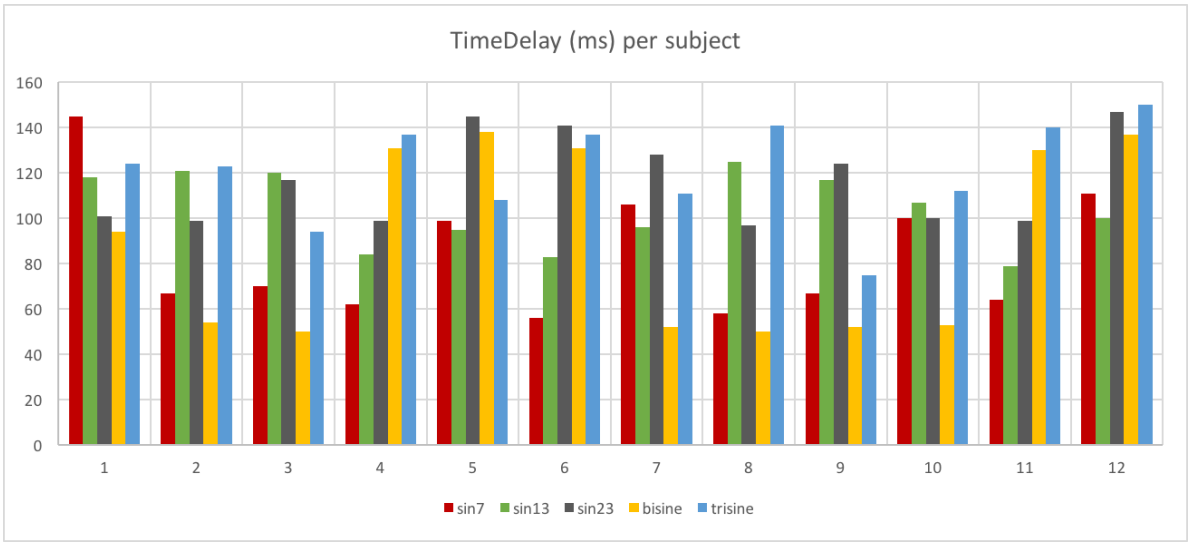

(a) Sines-Multisines

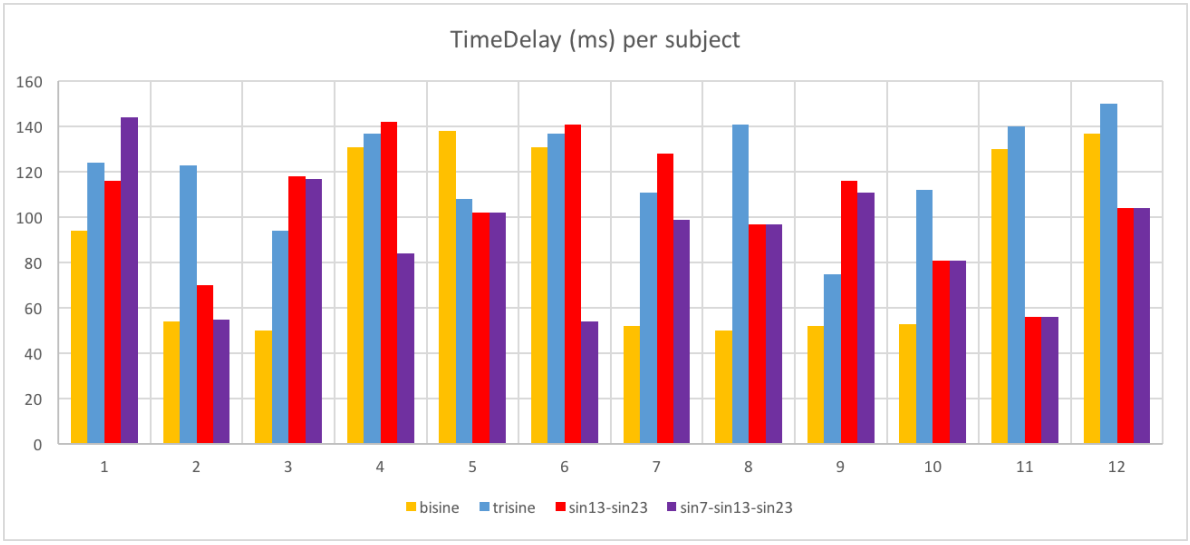

(b) Multisines-Combined Sines

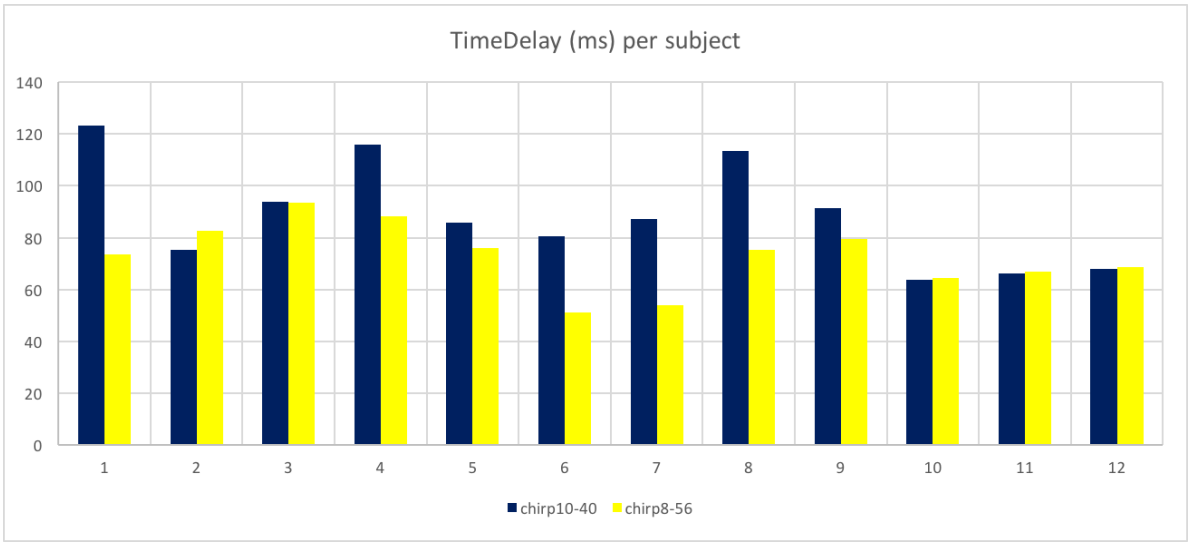

(c) Chirps

Fig. 9: Time Delay per subject for all stimulation paradigms. Each column of he horizontal axis represent a participant. The vertical axis represents the time delay in milliseconds. The selected channel is POz.

IV. Discussion-Conclusions

This study investigated the nonlinear interactions and time delay in the visual pathway, using several types of stimulation paradigms. The assessment for the stable frequency sinusoidal paradigms was done using multi-spectral phase coherence (MSPC), a novel cross-frequency, amplitude-independent phase coupling measure [10]. On the other hand, the assessment for the chirp was done by taking consideration only the linear components of the signal. First we compared the brain activation and time delays between the sinusoidal signals and then we compared the time delays between the chirp signals. The conclusions of this study can be summarized to:

- Multisine paradigms activate the brain more localized than sine and chirp paradigms.
- Both multisine and chirp paradigms present clustering of time delays either in two or in three clusters.
- Bisine stimulation leads to highly separable time delay clusters, while trisine stimulation appears to lead in more accurate time delay estimation.
- Multisines and the respective combines sines have substantial differences in time delay estimation, due to the nonlinearity (intermodulation components that are taken into consideration) of the visual system.

A. (Multi)sines

1) Brain Activation: Harmonic and intermodulation phase coupling of second and third order was detected between all stimulation (multi)sines and the EEG. This result is in line with the reported nonlinear interactions in the visual pathway [12][19][30]. An indication on the localization of those interactions, showing that the visual associated areas are being activated is also in consonance with previous studies [31][32].

In all multi(sines) paradigms, fundamental frequency stimulation leads to the activation of the occipital cortex while higher order components activate the region between parietal and occipital cortex. These findings are in line with Pastor et al. (2007) [32] study proving that the origin of brain activation differs among the fundamental and higher order components.

The activation of the brain components might be a result of what Vialatte et al. (2010), and before him Srinivasan et al. (2007), referred to as SSVEP propagation through dipoles [20][33]. According to that theory the propagation of SSVEP starts in visual cortex and then expands sequentially into more brain areas as depicted in figure 10.

In all (multi)sine stimulations the input frequencies are intersected with the frequencies of the brain rhythms, like alpha and beta, as Herrmann (2001) suggested [12]. In case of multisine paradigms the response is examined by taking into account the coupling among input frequencies, harmonics and intermodulation components. The existence of intermodulation phenomenon might result in comparatively larger coupling among the input and output frequencies than among the input frequencies and the brain rhythms. On the contrary, the lack of intermodulation for sine paradigms combined with the resonance phenomenon occurring between the harmonics and the frequencies of brain rhythms, as explained by Herrmann (2001), might result in correlated oscillations between the brain rhythms and the stimulation [12]. Hence, the correlated oscillations might lead to substantial nonlinear components across the whole brain and therefore the topoplots appeared to be less localized than in multisine paradigms. The more localized responses of multisine stimulation paradigms compared to the rest of the paradigms, could be an indication that the use of multisine is a proper and controllable way to study the light processing in visual system.

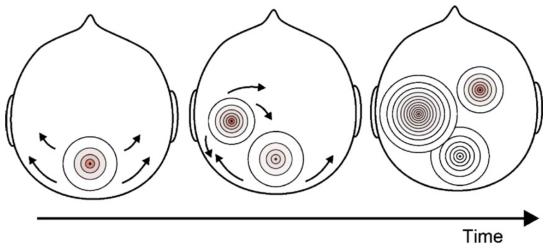

Fig. 10: Sequential SSVEP propagation starting from visual cortex and expanding in more regions [20].

2) Time Delay: Time delays were calculated and found to have high inter-subject and inter-stimulus variability. Although all stimulation types can be clustered, bisine is the stimulation that provides the most distinguishable clusters. Hence it seems to be a suitable and controllable way to help distinct between groups, especially in studies with neurological disorders where there is distinction and comparison between healthy controls and patients. On the other hand, trisine stimulation had the smallest inter-subject variability, indicating higher precision in time delay estimation.

3) Multisines vs Combined Sines: Considerable similarities in time delay estimation among multisines and the combined respective sines would mean that there is no need to apply all stimulation paradigms and hence the experimental time would decrease. Time delays, as they have been calculated, were found to be different. This was a rational finding since first, the visual system is highly nonlinear and therefore there is not proportional relation between the input and output; and second, in time delay estimation for multisines, intermodulation components are also taken into account, affecting thus the estimation.

B. Chirps

Chirp stimulation, a novel type of stimulation, was used to further measure the brain response of the visual and quantify the time delay between input and output. The selection of the specific frequency range was based on previous literature [22][23]. In consonance with Tu et al. (2011) the highest signal to noise ratio was found to be in the occipital region.

Chirp response was found to be very frequency dependent. From the two chirp signals, the response to 10-40 Hz seems to be more localized in terms of brain activation. A possible reason for that can be the fact that 10-40 Hz chirp consist of frequencies that are below the flicker frequency healthy

controls can perceive, also known as critical flicker frequency (CFF) or fusion flicker threshold (FFT) [34]. Above that threshold, which has reported to be around 44 Hz by Kowacs et al. (2005) [34], the individuals do not perceive flickering. Chirp 8-56 Hz consists of frequencies above the critical flicker frequency and hence the response might change above this specific limit. This can be a reason for less localized response than when used chirp 10-40 Hz.

Similar to multisine paradigms, the chirp time delays were clustered either in three or in two groups. This seems rational since according to Tu et al. (2011) chirp VEP is a generalization of SSVEP, and since there are frequency components that leads to clustering in SSVEP, there can be clustering in chirp VEP as well [22].

Chirp time delay has been found to be relatively smaller than time delays of the multisine paradigms. This seems logical since the brain needs to respond to a fast changing stimulus [23]. However, only the linear components are taken into account in the estimation of time delay. Therefore we should expect different time delays for chirps in case of consideration of the nonlinear parts.

C. Recommendations

The recommendations, based on the limitations we faced in this study, are:

1) Stimulation Artifact: The existed stimulation artifact in the half of the subjects may have affected the outcome of this study. According to our knowledge the replacement of the artifact region with linearly spaced points is a suitable method to overcome this limitation. The application of this method, as it is presented in Appendix A, provided us with trusted results.

2) Sample Size: The size of the sample was decent. Bisine and trisine stimulation presented the most interesting characteristics, as bisine seems to be a suitable distinction measure, while trisine seems to lead to an accurate time delay estimation. A larger sample would be a proper way to further examine those characteristic in order to make more concrete results. The age of the sample should also be taken into consideration since the age affects the boundaries of the three aforementioned components, the critical flicker frequency and the responses of the brain may changes. Therefore a sample with age groups may also provide important differences between the groups.

3) Motivation: The stimulation for all paradigms lasted one hour. Therefore the motivation and vigilance of the subject has probably decreased through this period. As a result, subjects may faced periods of lack of concentration and as a result increased eye movement. The artifacts occurred due to eye movement were rejected. However, some of the unwanted information may have not been removed and may have minimal effect to the result of this study. Fewer stimulation paradigms could decrease the experimental time and provide increased vigilance.

4) Eye blinks in chirp stimulation: Chirp responses consists of the same frequency range as the stimulus. During eye blinks the responses are disrupted. Hence, there might be frequency discontinuities that can affect the analysis. To overcome this limitation, we recommended and applied small blocks with rest in between that helped the participants to regain their concentration and vigilance, minimizing thus the possibility of eye blinking during the stimulation.

REFERENCES

[1] L. A. Remington, "Visual System," in *Clinical Anatomy and Physiology of the Visual System*, pp. 1–9, 2012.

[2] L. A. Remington, "Visual Pathway," in *Clinical Anatomy and Physiology of the Visual System*, pp. 233–252, 2012.

[3] F. Varela, J.-P. Lachaux, E. Rodriguez, and J. Martinerie, "The brainweb: phase synchronization and large-scale integration," *Nature reviews neuroscience*, vol. 2, no. 4, pp. 229–239, 2001.

[4] J.-M. Schoffelen, R. Oostenveld, and P. Fries, "Neuronal coherence as a mechanism of effective corticospinal interaction," *Science*, vol. 308, no. 5718, pp. 111–113, 2005.

[5] S. F. Campfens, A. C. Schouten, M. J. van Putten, and H. van der Kooij, "Quantifying connectivity via efferent and afferent pathways in motor control using coherence measures and joint position perturbations," *Experimental brain research*, vol. 228, no. 2, pp. 141–153, 2013.

[6] R. Shapley, "Linear and nonlinear systems analysis of the visual system: Why does it seem so linear?. A review dedicated to the memory of Henk Spekreijse," *Vision Research*, vol. 49, no. 9, pp. 907–921, 2009.

[7] M. Ahmadlou and H. Adeli, "Functional community analysis of brain: A new approach for EEG-based investigation of the brain pathology," *NeuroImage*, vol. 58, no. 2, pp. 401–408, 2011.

[8] C.-C. Chen, J. M. Kilner, K. J. Friston, S. J. Kiebel, R. K. Jolly, and N. S. Ward, "Nonlinear Coupling in the Human Motor System," *Journal of Neuroscience*, vol. 30, pp. 8393–8399, jun 2010.

[9] P. Sauseng and W. Klimesch, "What does phase information of oscillatory brain activity tell us about cognitive processes?," 2008.

[10] Y. Yang, T. Solis-Escalante, J. Yao, A. Daffertshofer, A. C. Schouten, and F. C. T. van der Helm, "A General Approach for Quantifying Nonlinear Connectivity in the Nervous System Based on Phase Coupling.," *International journal of neural systems*, vol. 26, no. 1, p. 1550031, 2015.

[11] K. J. Friston, "The labile brain. i. neuronal transients and nonlinear coupling.," *Philosophical Transactions of the Royal Society B: Biological Sciences*, vol. 355, no. 1394, p. 215, 2000.

[12] C. S. Herrmann, "Human EEG responses to 1-100 Hz flicker: Resonance phenomena in visual cortex and their potential correlation to cognitive phenomena," *Experimental Brain Research*, vol. 137, no. 3-4, pp. 346–353, 2001.

[13] X. Chen, Z. Chen, and S. Gao, "Brain-computer interface based on intermodulation frequency.," *Journal of neural engineering*, vol. 10, p. 066009, dec 2013.

[14] M. Cheng, X. Gao, S. Gao, and D. Xu, "Multiple color stimulus induced steady state visual evoked potentials," *2001 Conference Proceedings of the 23rd Annual International Conference of the IEEE Engineering in Medicine and Biology Society*, vol. 2, pp. 1012–1014, 2001.

[15] M. P. Regan and D. Regan, "A frequency domain technique for characterizing nonlinearities in biological systems," *Journal of Theoretical Biology*, vol. 133, no. 3, pp. 293–317, 1988.

[16] P. Husar and G. Henning, "Bispectrum analysis of visually evoked potentials," *IEEE Engineering in Medicine and Biology Magazine*, vol. 16, no. 1, pp. 57–63, 1997.

[17] Y. Yang, T. Solis-Escalante, F. Van der Helm, and A. Schouten, "A Generalized Coherence Framework for Detecting and Characterizing Nonlinear Interactions in the Nervous System," *IEEE Transactions on Biomedical Engineering*, pp. 1–1, 2016.

[18] J. D. Victor and R. Shapley, "A method of nonlinear analysis in the frequency domain," *Biophysical Journal*, vol. 29, pp. 458–483, mar 1980.

[19] A. M. Norcia, L. G. Appelbaum, J. M. Ales, B. R. Cottereau, and B. Rossion, "The steady-state visual evoked potential in vision research: A review.," *Journal of vision*, vol. 15, p. 4, may 2015.

[20] F. B. Vialatte, M. Maurice, J. Dauwels, and A. Cichocki, "Steady-state visually evoked potentials: Focus on essential paradigms and future perspectives," *Progress in Neurobiology*, vol. 90, no. 4, pp. 418–438, 2010.

[21] D. Regan, "A high frequency mechanism which underliers VEP," *Electroencephalography and clinical Neurophysiology*, vol. 25, no. 3, pp. 231–237, 1968.

[22] T. Tu, Y. Xin, X. Gao, and S. Gao, "Chirp-modulated visual evoked potential as a generalization of steady state visual evoked potential," *Journal of Neural Engineering*, vol. 9, p. 016008, 2011.

[23] A. R. Gantenbein, P. S. Sandor, P. J. Goadsby, and H. Kaube, "Chirp stimulation: H-response short and dynamic.," *Cephalalgia : an international journal of headache*, vol. 0, no. 0, pp. 1–5, 2014.

[24] M. Vlaar, T. Solis-Escalante, A. Vardy, F. Van der Helm, and A. Schouten, "Quantifying nonlinear contributions to cortical responses evoked by continuous wrist manipulation," *IEEE Transactions on Neural Systems and Rehabilitation Engineering*, 2016.

[25] P. M. Milner, "A model for visual shape recognition.," *Psychological review*, vol. 81, no. 6, p. 521, 1974.

[26] R. B. Silberstein, J. Ciorciari, and A. Pipingas, "Steady-state visually evoked potential topography during the Wisconsin card sorting test.," *Electroencephalography and clinical neurophysiology*, vol. 96, no. 1, pp. 24–35, 1995.

[27] S. L. Peng, Y. Xin, F. Y. Tian, S. K. Liu, and a. L. F. M. Signal, "Detection of Linear Frequency Modulated Flash Visual Evoked Potential by Fractional Fourier Transform," no. Aiie, pp. 429–432, 2015.

[28] L. B. Almeida, "The Fractional Fourier Transform and Time-Frequency Representations," *IEEE Transactions on Signal Processing*, vol. 42, no. 11, pp. 3084–3091, 1994.

[29] D. Regan, "Human brain electrophysiology: evoked potentials and evoked magnetic fields in science and medicine," 1989.

[30] D. Zhu, J. Bieger, G. Garcia Molina, and R. M. Aarts, "A survey of stimulation methods used in SSVEP-based BCIs," *Computational Intelligence and Neuroscience*, vol. 2010, 2010.

[31] M. a. Pastor, J. Artieda, J. Arbizu, M. Valencia, and J. C. Masdeu, "Human cerebral activation during steady-state visual-evoked responses.," *The Journal of neuroscience : the official journal of the Society for Neuroscience*, vol. 23, no. 37, pp. 11621–11627, 2003.

[32] M. A. Pastor, M. Valencia, J. Artieda, M. Alegre, and J. C. Masdeu, "Topography of cortical activation differs for fundamental and harmonic frequencies of the steady-state visual-evoked responses. An EEG and PET H 215O study," *Cerebral Cortex*, vol. 17, no. 8, pp. 1899–1905, 2007.

[33] R. Srinivasan, W. R. Winter, J. Ding, and P. L. Nunez, "Eeg and meg coherence: measures of functional connectivity at distinct spatial scales of neocortical dynamics," *Journal of neuroscience methods*, vol. 166, no. 1, pp. 41–52, 2007.

[34] P. A. Kowacs, E. J. Piovesan, L. C. Werneck, H. Fameli, A. C. Zani, and H. P. Da Silva, "Critical flicker frequency in migraine. A controlled study in patients without prophylactic therapy," *Cephalalgia*, vol. 25, no. 5, pp. 339–343, 2005.

APPENDIX A
ARTIFACT

The (pre)processing of each participant was taking place while new participants were recorded. Therefore the presence of the artifact in the first six participants were discovered early in the experimental process. After many test experiments we found out that the triggers signal that was captured by one of the auxiliary ports of the amplifier had very high amplitude and due to improper insulation of the amplifier, the electrodes above that port were highly affected. Therefore for the rest of the experiments the amplitude of the trigger signal was decreased by a factor of 1000. This change prevented further contamination of the EEG signals.

The following step was to find a way to remove the artifact from the contaminated subjects and linear interpolation of the samples before and after the artifact seemed the best solution. However we should first decide if the replacement of the artifact with linear points would have an effect in the parameters we wanted to measure (phase difference, frequency, time delay). To make such a decision, we checked how the parameters change if we linearly interpolate the first 25 samples of a participant without the artifact with respect to the same participant's raw EEG data. The conclusion from this process was that the replacement of the artifact region using linearly spaced points does not affect our parameters in a high degree. Figures of test examples can be seen below verifying our conclusion.

Figure 11 a shows how the replacement of the artifact region affected a contaminated subject. It can be seen that frequencies, phase difference and as a conclusion time delay are totally different. Figures 11 b,c,d show how the replacement of the first 25 samples in a not contaminated subject didn't affect at all or affect in a very small degree the desired parameters. The aforementioned conclusions are valid for all the subjects and stimulation paradigms but are not presented in this report.

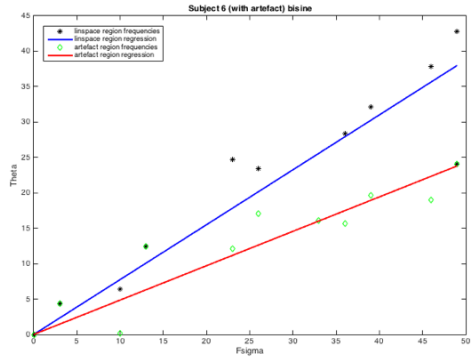

(a) Contaminated Subject

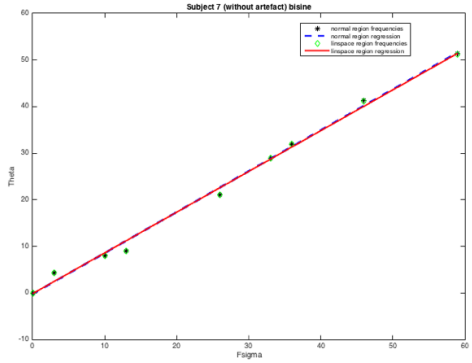

(b) Not Contaminated Subject Bisine

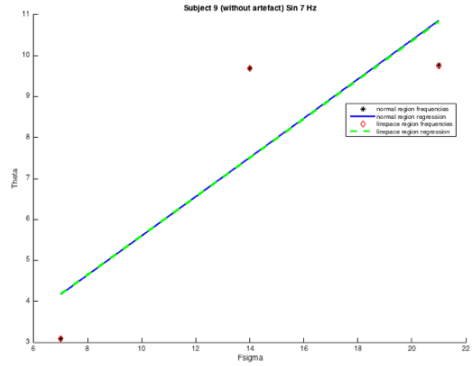

(c) Not Contaminated Subject bisine Sine7

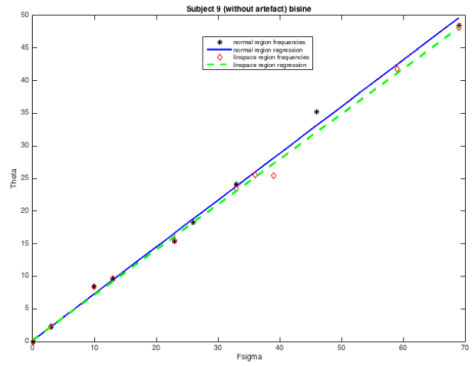

(d) Another Not Contaminated Subject Bisine

Fig. 11: MSPC frequencies and phase difference for contaminated and not contaminated representative subjects and stimulation paradigms

APPENDIX B
AVERAGED SNR PLOTS PER STIMULATION TYPE

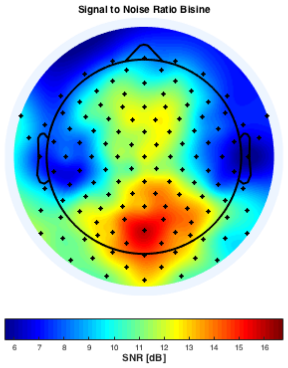

(a) Bisine

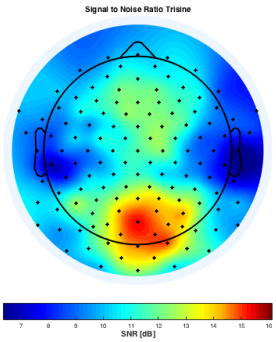

(b) Trisine

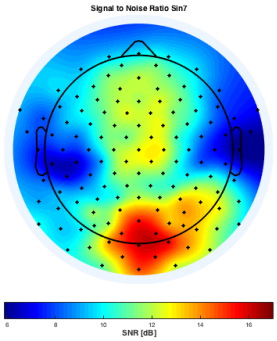

(c) sine 7

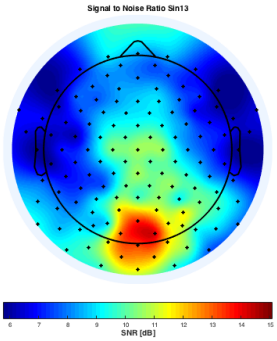

(d) sine 13

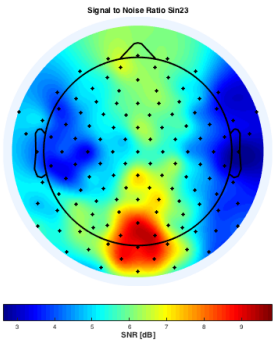

(e) sine 23

Fig. 12: Signal to noise ratio (SNR) per electrode averaged over all subjects. The highest SNR is found between parietal and occipital brain regions. The dots indicate the electrodes' locations.

APPENDIX C
AVERAGED MSPC PLOTS PER STIMULATION TYPE

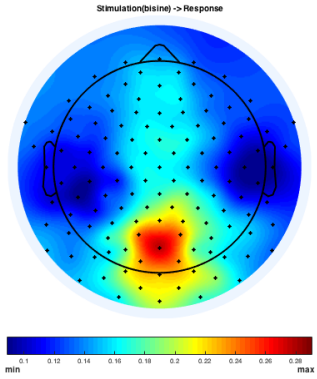

(a) Bisine

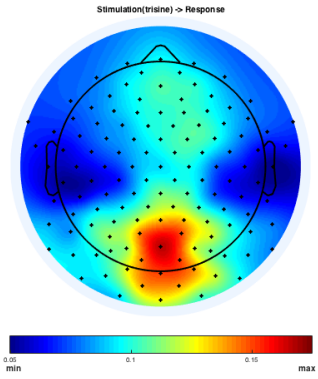

(b) Trisine

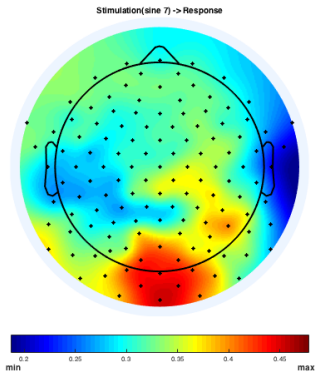

(c) sine 7

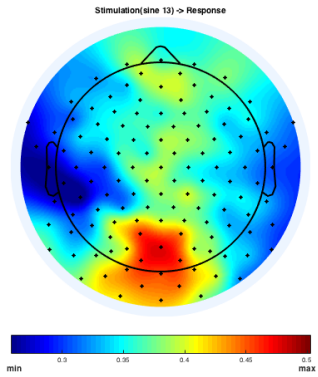

(d) sine 13

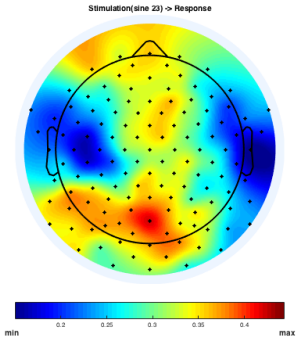

(e) sine 23

Fig. 13: Scalp topography of the mean MSPC significant $\Psi_{stimulation \rightarrow EEG}$. Black dots indicate the electrodes' locations.

APPENDIX D
MSPC SIGNIFICANT VALUES

A. *Bisine Subjects 1-6*

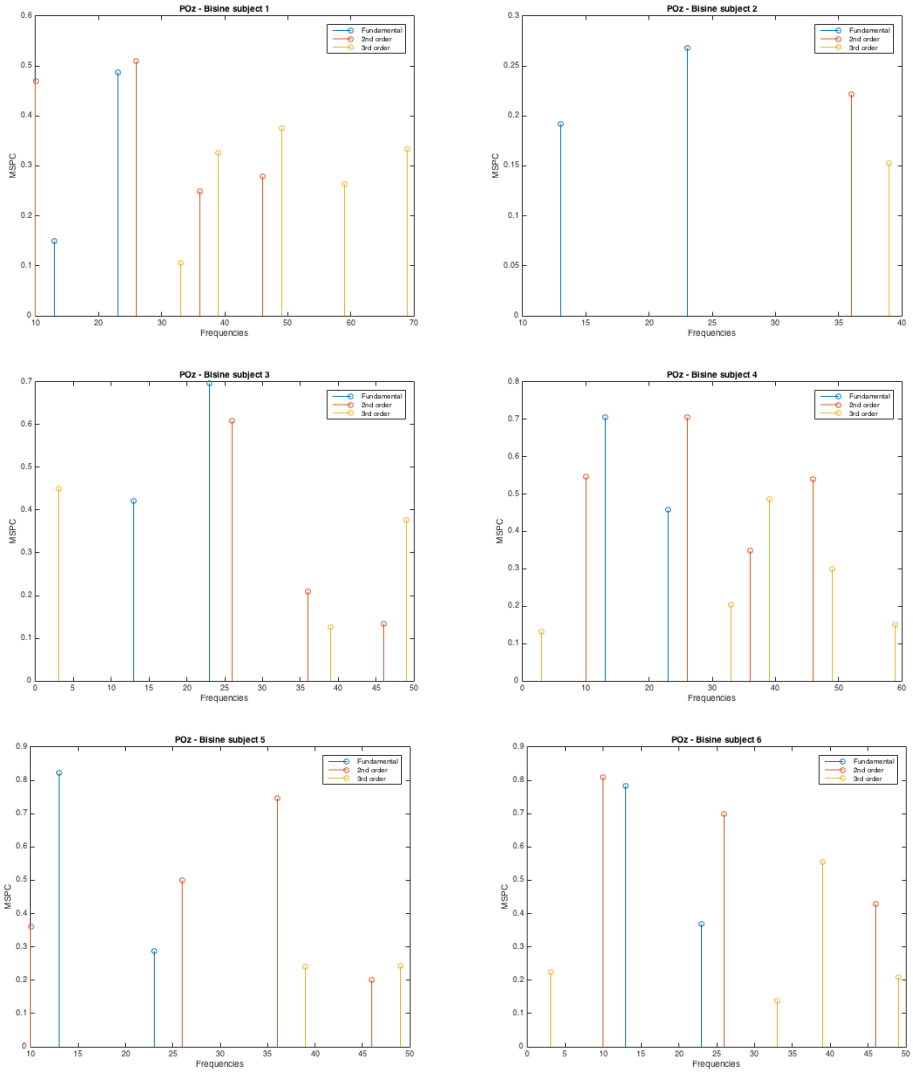

Fig. 14: Nonlinear significant interactions for subjects 1-6 using bisine stimulation

B. Bisine Subjects 7-12

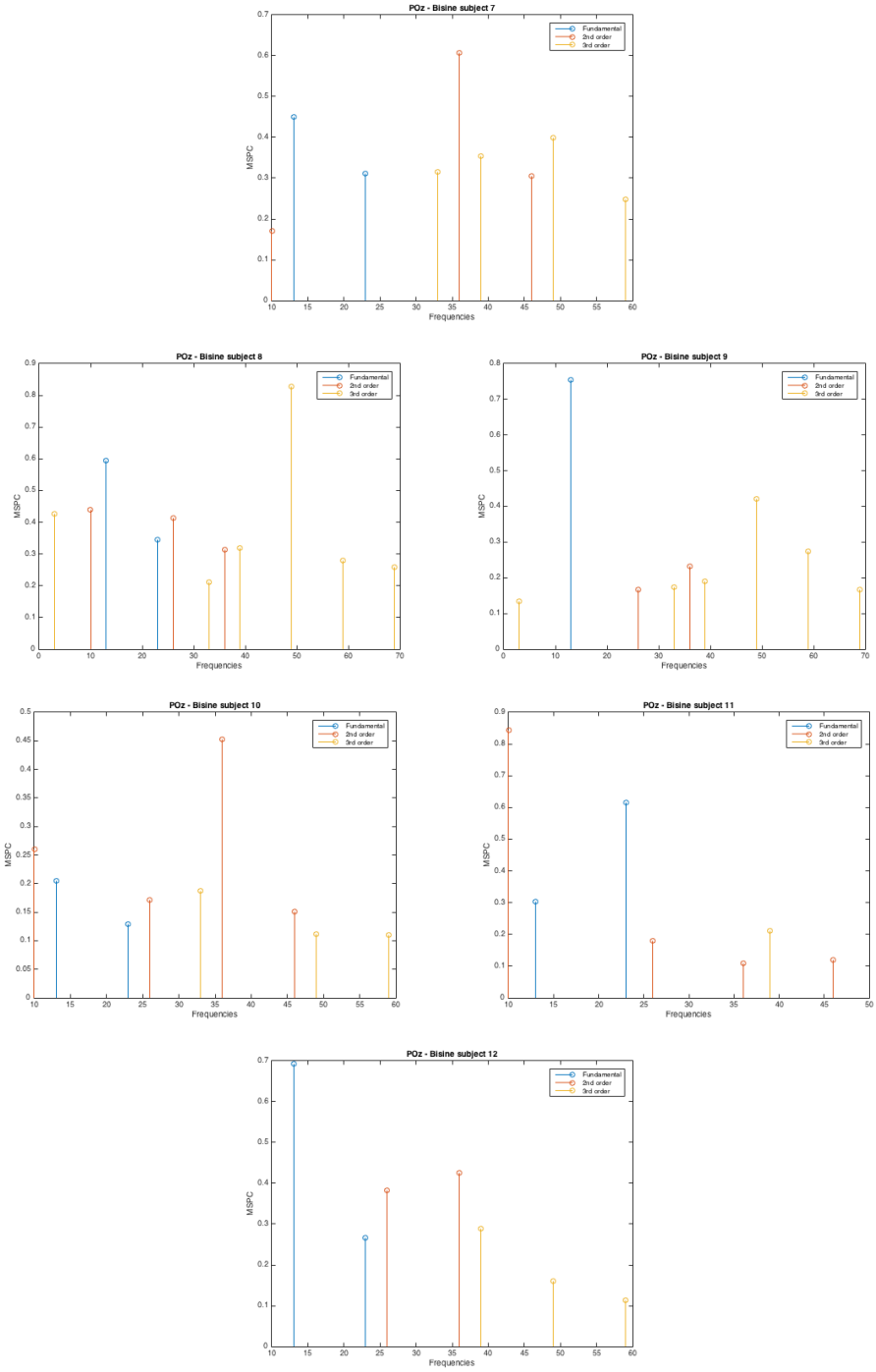

Fig. 15: Nonlinear significant interactions for subjects 7-12 using bisine stimulation

C. Trisine Subjects 1-6

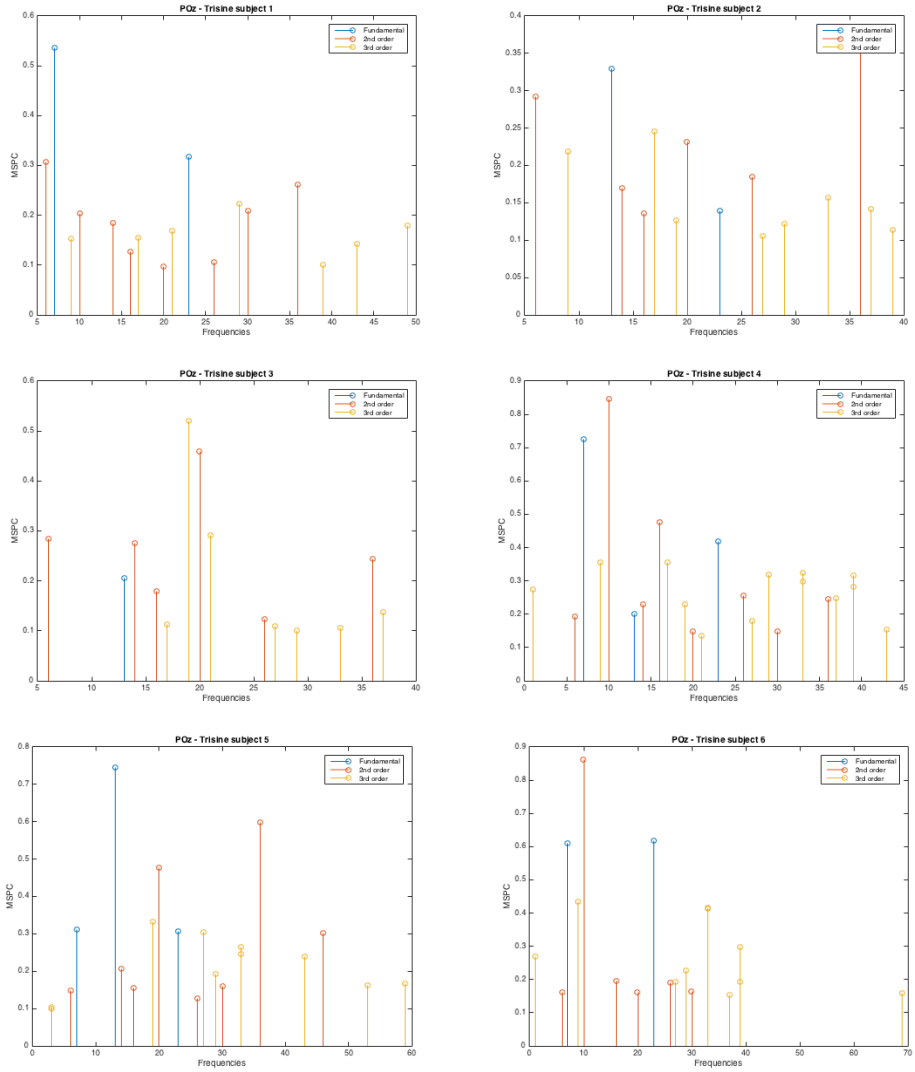

Fig. 16: Nonlinear significant interactions for subjects 1-6 using bisine stimulation

D. Trisine 7-12

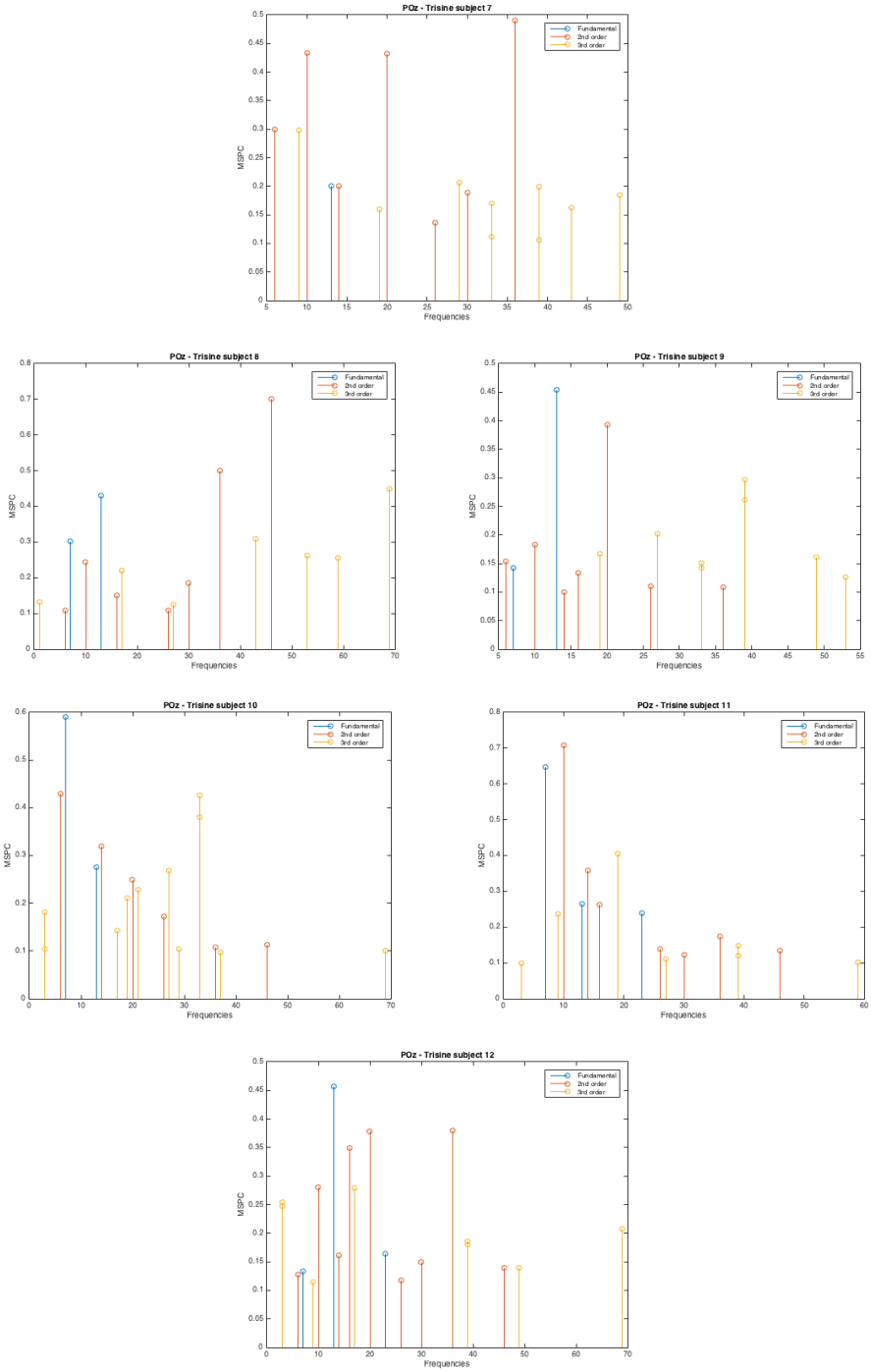

Fig. 17: Nonlinear significant interactions for subjects 7-12 using bisine stimulation

E. Mean-STD MSPC

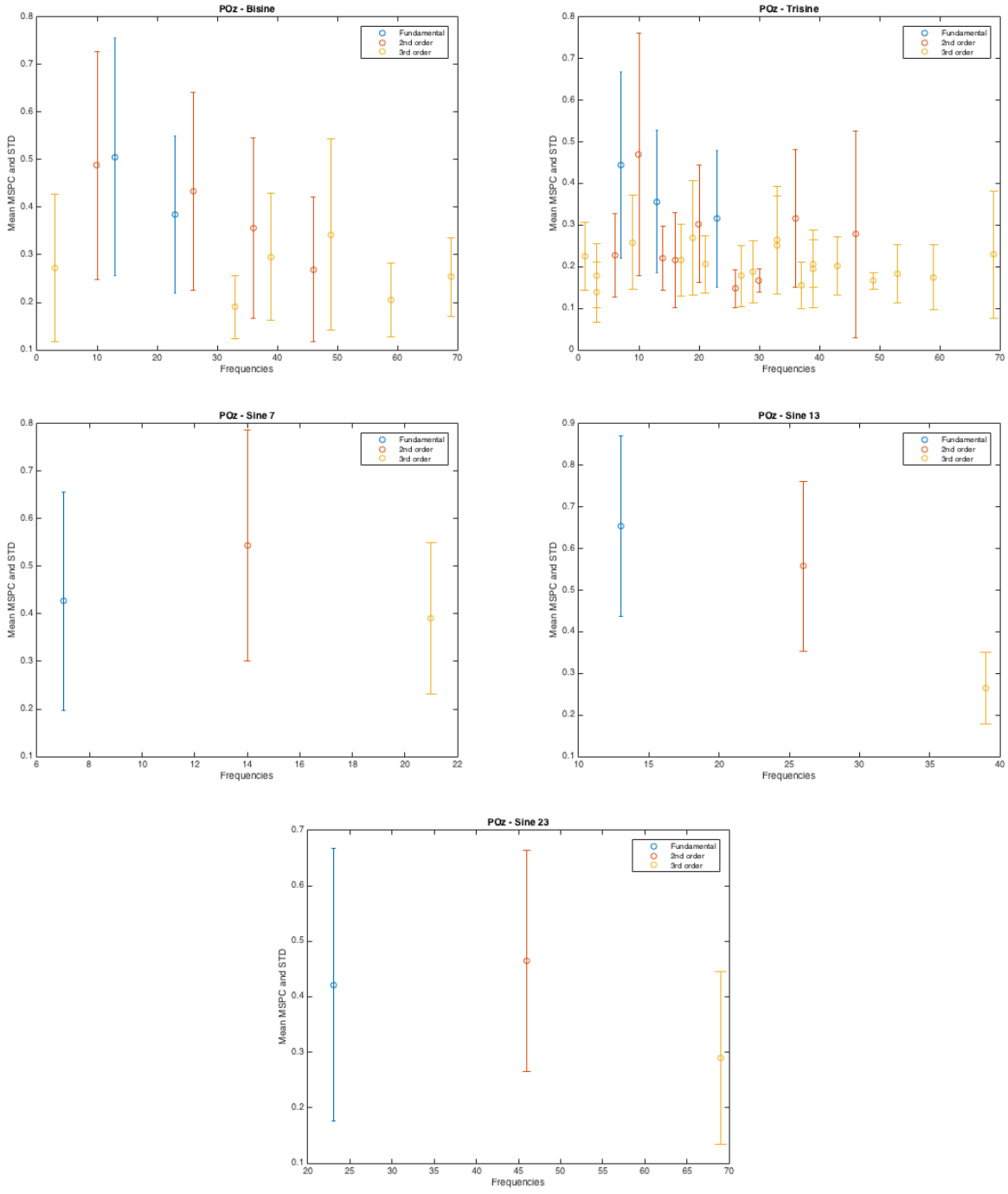

Fig. 18: Mean and STD of MSPC over all subjects

F. Mean-SEM MSPC

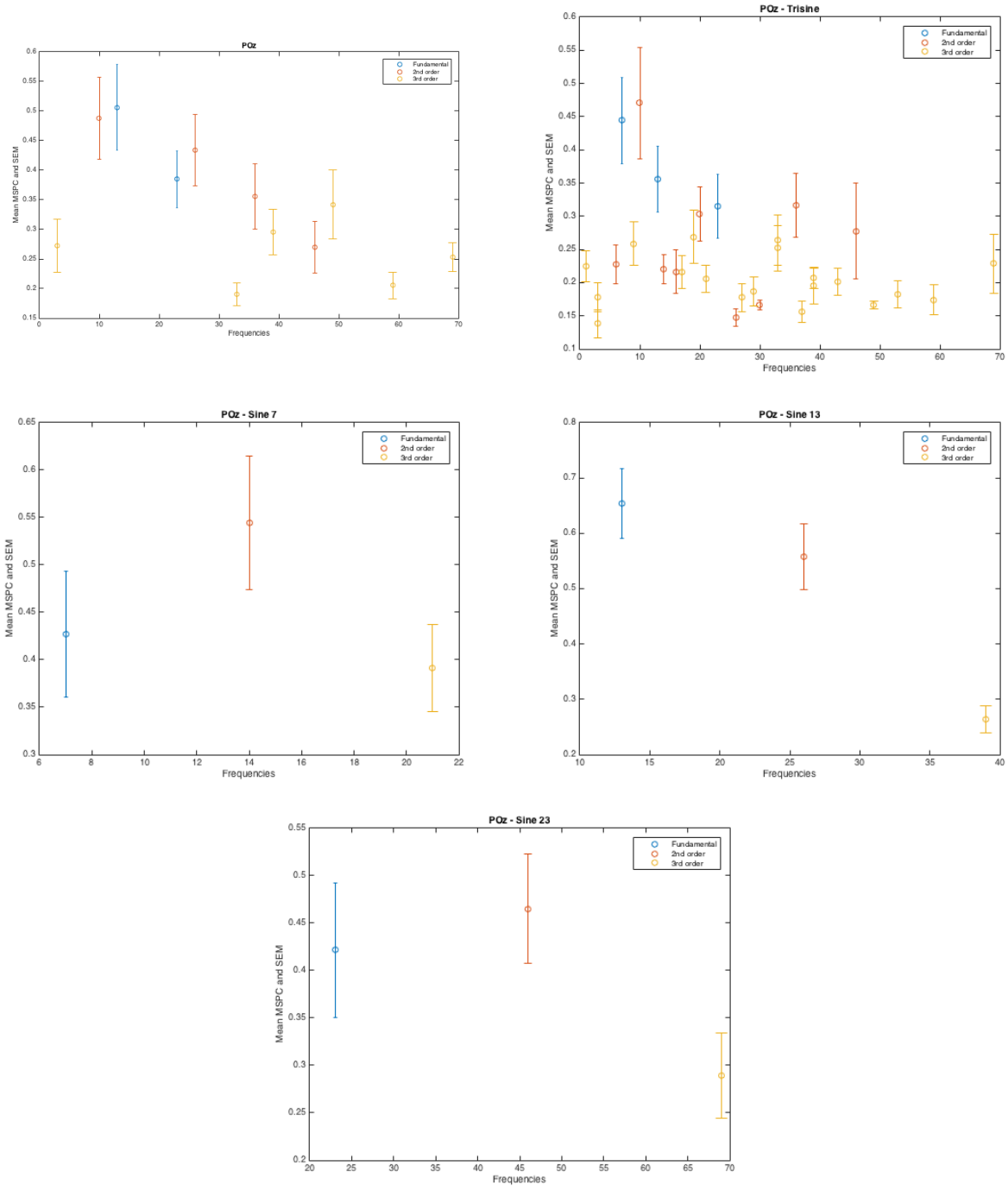

Fig. 19: Mean and SEM of MSPC over all subjects

APPENDIX E
AVERAGED MSPC PLOTS PER MULTISINE PER ORDER

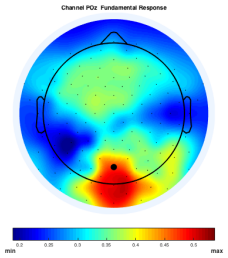

(a) Bisine Fundamental

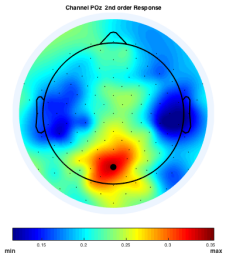

(b) Bisine 2nd order

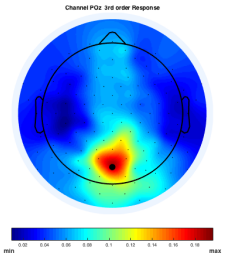

(c) Bisine 3rd order

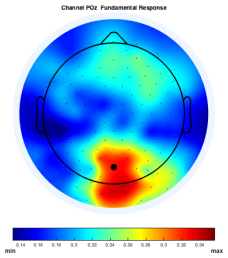

(d) Trisine Fundamental

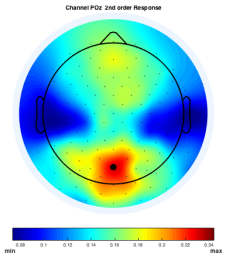

(e) Trisine 2nd order

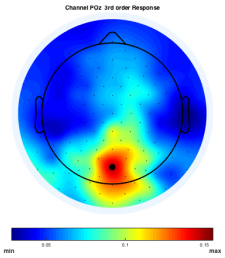

(f) Trisine 3rd order

Fig. 20: Scalp topography of the mean MSPC significant $\Psi_{stimulation \rightarrow EEG}$ per order. Each row represents a multisine. Each column represents a different order. Black dots indicate the electrodes' positions. Filled black dot represents POz electrode.

APPENDIX F
AVERAGED MSPC PLOTS PER SINE PER ORDER

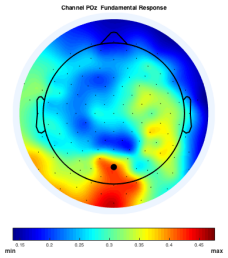

(a) Sine 7 Fundamental

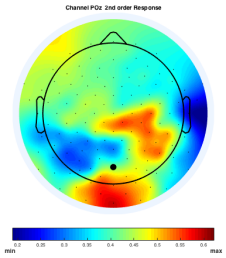

(b) Sine 7 2nd order

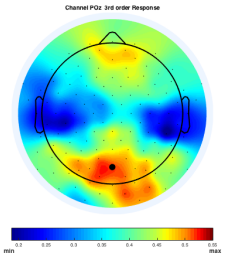

(c) Sine 7 3rd order

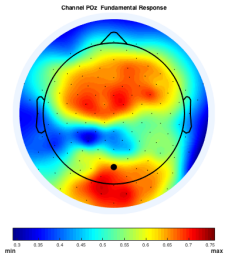

(d) Sine 13 Fundamental

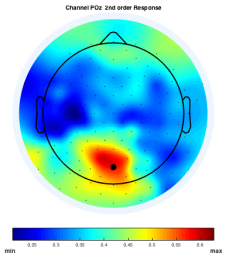

(e) Sine 13 2nd order

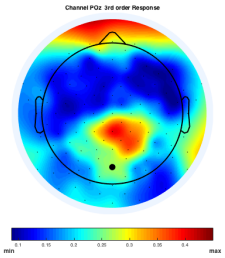

(f) Sine 13 3rd order

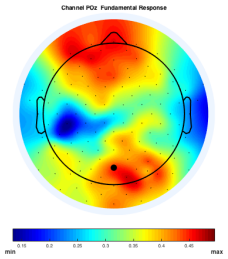

(g) Sine 23 Fundamental

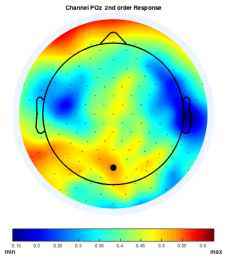

(h) Sine 23 2nd order

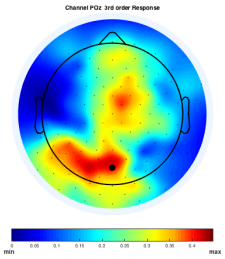

(i) Sine 23 3rd order

Fig. 21: Scalp topography of the mean MSPC significant $\Psi_{stimulation \rightarrow EEG}$ per order. Each row represents a sine. Each column represents a different order. Black dots indicate the electrodes' positions. Filled black dot represents POz electrode.

APPENDIX G
MSPC VS TIMEDELAY CLUSTERING

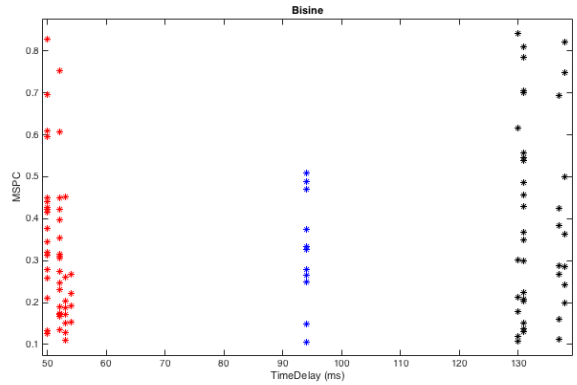

(a) Bisine

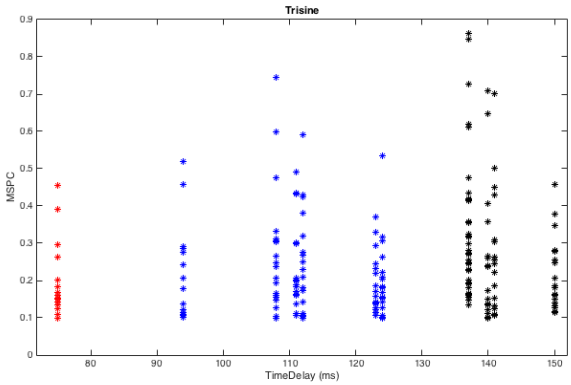

(b) Trisine

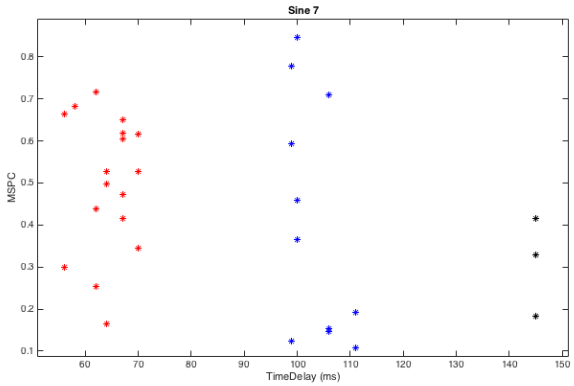

(c) Sine7

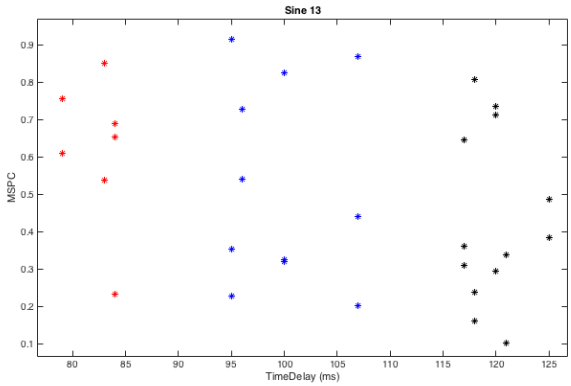

(d) Sine13

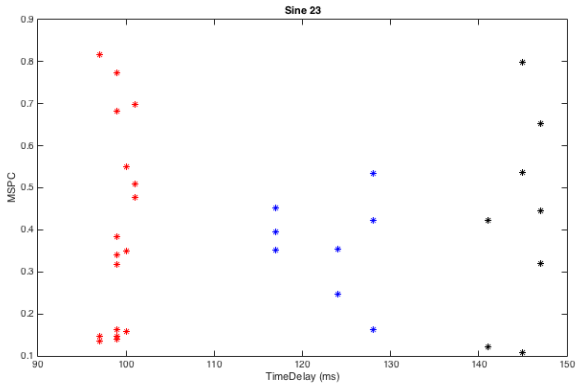

(e) Sine23

Fig. 22: MSPC values of all subjects contributing in the formation of three clusters for all (multi)sines paradigms.

APPENDIX H
MSPC VS TIMEDELAY - THREE COMPONENTS

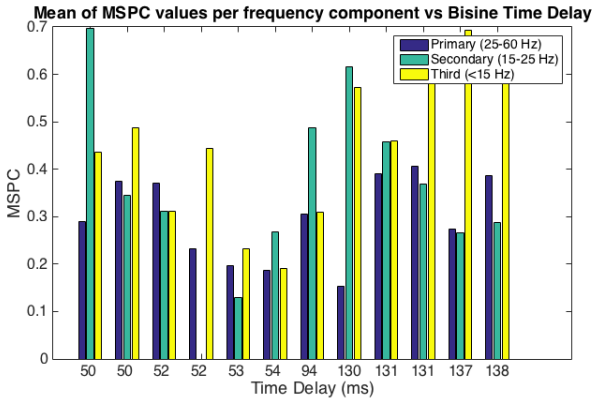

(a) Bisine

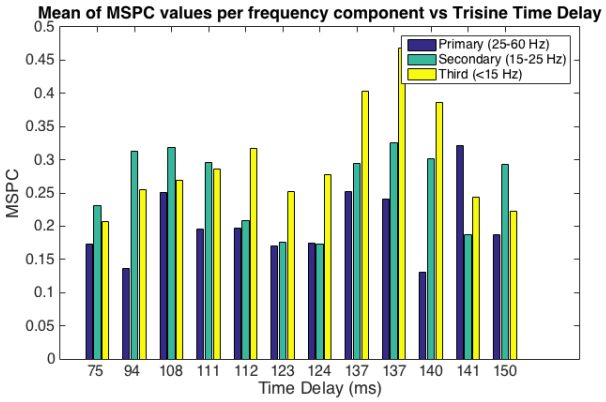

(b) Trisine

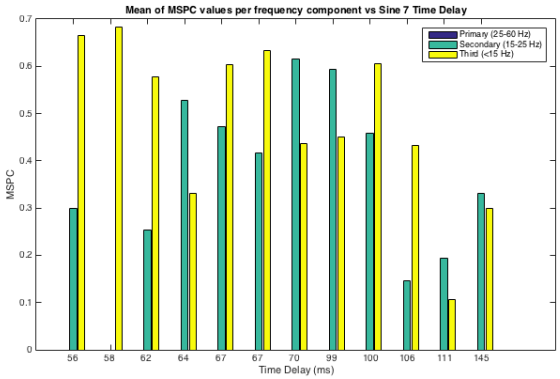

(c) Sine7

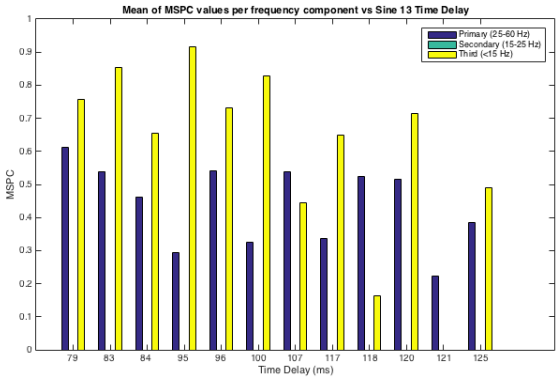

(d) Sine13

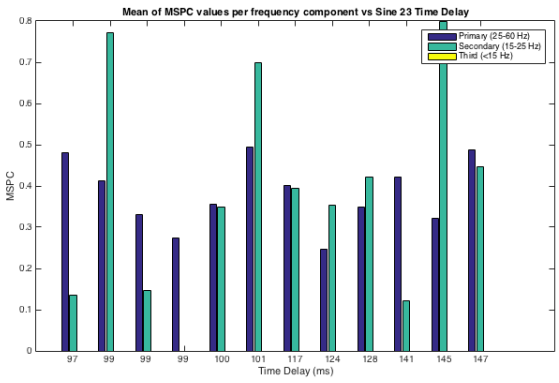

(e) Sine23

Fig. 23: Mean MSPC for each frequency component for (multi)sine stimulations